Composition and Temperature Dependence of Terminal and Segmental Dynamics in Polyisoprene/Poly(vinylethylene) Blends

Jeffrey C. Haley and Timothy P. Lodge*,†

Department of Chemical Engineering and Materials Science, University of Minnesota, Minneapolis, Minnesota 55455

Yiyong He and M. D. Ediger*

Department of Chemistry, University of Wisconsin−Madison, Madison, Wisconsin 53706

Ernst D. von Meerwall

Department of Physics and Maurice Morton Institute of Polymer Science, University of Akron, Akron, Ohio 44325

Jovan Mijovic

Department of Chemical Engineering and Chemistry and the Herman F. Mark Polymer Research Institute, Polytechnic University, Six MetroTech Center, Brooklyn, New York 11201

Received April 2, 2003; Revised Manuscript Received June 9, 2003

ABSTRACT: The frequency-dependent shear moduli were measured over a range of temperature for polyisoprene (PI, $M = 22\,000$ and 78 000), poly(vinylethylene) (PVE, $M = 10\,000$ and 120 000), and their blends. The longest relaxation times of each component in the blends were extracted by a modified Tsenoglou mixing rule, and converted to monomeric friction factors via the reptation model. Dielectric relaxation and pulsed field gradient NMR were used to follow the terminal relaxation and diffusion, respectively, of a low molecular weight PI ($M = 1300$) in blends with perdeuterated PVE ($M = 2300$), for a range of temperature and composition. In this case monomeric friction factors were extracted via the Rouse model. The friction factors for PI via all three techniques agreed quantitatively, and the friction factors for both components were independent of molecular weight. Segmental dynamics of each component in PI/PVE blends by NMR methods, reported in the literature, could be compared directly with the terminal relaxation data. In all cases, the segmental and terminal dynamics exhibited equivalent dependences on temperature and composition. The predictions of the model of Lodge and McLeish were compared to the combined data, by calculating component self-concentrations and effective glass transition temperatures using a single temperature-independent length scale. As anticipated in the original model, this length scale is close to the Kuhn length of the particular component. In the case of PI, the model provides a quantitative description over the entire composition and temperature range studied. For PVE the agreement is not as quantitative, but it is still quite satisfactory.

Introduction

The dynamics of polymer mixtures are important in understanding a wide range of phenomena, including the kinetics of phase separation, the rheological response of block copolymers, and the processing of polymer blends. In each of these areas, the macroscopic response reflects the combined contributions of the components; it is therefore important to understand not only the "mixing rules" that determine the macroscopic response but also the dynamics of the individual components in the mixture as functions of composition and temperature. Miscible polymer blends can serve as model systems for resolving the dynamics of the individual components and provide a convenient route to examining the relationships between terminal and segmental dynamics in polymer mixtures.

Miscible polymer blends exhibit several well-documented dynamic "anomalies". The time−temperature superposition principle that is generally successful in homopolymers has been shown to fail for several blend systems,[1−5] and unusually broad calorimetric glass transitions have been commonly observed.[3,4,6] Measurements of the tracer diffusion of each component in a blend have revealed surprisingly complex dependences of the monomeric friction factor (ζ) on temperature and composition.[7−9] These results, and others, are consistent with the hypothesis that each component experiences its own distinct "effective" glass transition temperature ($T_{g,eff}$),[10] which generally differs from both the glass transition temperatures (T_g) of the pure homopolymers and the mean T_g of the blend.

This thermorheological complexity is likely due to a combination of factors, including intrinsic differences in mobility between the components, and local variations in composition that contribute to $T_{g,eff}$. At least three distinct (but not necessarily mutually exclusive) approaches have been developed to describe the compositional heterogeneity of miscible polymer blends. One emphasizes the self-concentration, the local enrichment in the environment of a particular monomer with monomers from the same chain, due to chain connectivity.[11−13] Lodge and McLeish proposed that the relevant length scale for determining segmental dynamics and the

* Authors for correspondence: T.P.L., lodge@chem.umn.edu; M.D.E., ediger@chem.wisc.edu.
† Also at the Department of Chemistry, University of Minnesota, Minneapolis, MN 55455.

10.1021/ma034414z CCC: $25.00
Published on Web 07/19/2003

effective glass transition temperature is approximately the Kuhn length of the chain. Thus, stiffer polymers respond to the local environment in a relatively larger volume, leading to smaller self-concentration effects. This approach is potentially a predictive scheme, in that if $\zeta(T)$ and the Kuhn length are known for the pure components, the composition and temperature dependence of the segmental dynamics in any mixture can be calculated. Furthermore, if the relationship between segmental dynamics and terminal dynamics is the same in the blend as it is for the pure components, then both the terminal and segmental dynamics can be described with no new parameters. One alternative approach combines the cooperatively rearranging region concept of Adam and Gibbs, a postulated divergence of this volume as the glass transition is traversed, and concentration fluctuations within this volume given by the random-phase approximation.[14−17] This formulation requires additional specification of the cooperative volume, its temperature dependence, and the static structure factor. Another approach extends the coupling model, in which cooperativity between different molecules leads to stretched exponential relaxation functions.[18] In miscible blends, each component exhibits a distribution of "stretching exponents", attributed to a distribution of local environments.[19,20]

Polyisoprene (PI) and poly(vinylethylene) (PVE) form an attractive system for studies of miscible blend dynamics. Both PI and PVE can be synthesized via anionic polymerization, resulting in narrow distribution polymers. A wealth of information about the dynamics of PI/PVE blends is already available, as this blend has been studied by rheology,[4,21,22] rheo-optics,[23−25] dielectric relaxation,[16,21,26] and quasielastic neutron scattering.[26,27] Substantial segmental relaxation data are available from NMR measurements,[11,28,29] data that are of particular use in comparing terminal and segmental dynamics. Additionally, PI and PVE are miscible over a wide range of temperatures and compositions and form a nearly athermal blend.[30] Thus, enthalpic effects are not expected to have a significant impact on the dynamics. In this paper, we describe measurements of the terminal dynamics of PI/PVE blends using pulsed-gradient spin echo NMR, dielectric relaxation, and rheology. The dynamic behavior of each blend component was studied at several compositions over a temperature interval extending over almost 200 K. The resulting data are compared with published segmental dynamics results and establish that the relationship between terminal and segmental dynamics in these blends is the same as that in the pure components. The data are also compared with the predictions of the self-concentration model of Lodge and McLeish.

Experimental Section

Materials Synthesis and Characterization. The low molecular weight samples PI-1 and PVE-2 were synthesized through anionic polymerization; the numerical designation corresponds to the number-average molecular weight in kg/mol, and PVE-2 is perdeuterated. Details regarding the purification, synthesis and characterization of these materials are available elsewhere.[29,31] The same blend samples (PI-1/PVE-2: 100/0, 70/30, 50/50, 30/70, 0/100 percent by weight) were used in NMR relaxation,[29] pulsed-gradient spin echo NMR (PGSE), and the dielectric relaxation (DR) measurements.

The higher molecular weight PI-22, PI-78, PVE−10, and PVE−120 samples used in the rheology experiments were also prepared by anionic polymerization. Cyclohexane (solvent) was purified by passing through alumina and silica columns. Isoprene was degassed and stored on calcium hydride. The purification of isoprene and butadiene was accomplished by stirring for 4 h over dibutylmagnesium followed by 4 h over *n*-butyllithium. Ethylene oxide (terminating agent) was purified by stirring for 1 h over dibutylmagnesium. 1,2-Dipiperidinoethane (structural modifier) was purified by stirring over calcium hydride for several days. The concentration of *sec*-butyllithium (initiator) was determined by the Gilman double-titration method.[32]

Table 1. Characteristics of PI and PVE Homopolymers

samples	M_n (kg/mol)	M_w/M_n	T_g (K)	% microstructure *cis*-1,4	*trans*-1,4	3,4
PI-1	1.35[a]	1.11[b]	201	61[c]	24[c]	15[c]
PI-22	22[d]	1.03[d]	211		93[e]	7[e]
PI-78	78[d]	1.02[d]	212		95[e]	5[e]

samples	M_n (kg/mol)	M_w/M_n	T_g (K)	% microstructure 1,2	1,4
PVE-2[f]	2.35[a]	1.05[b]	260	94[c]	6[c]
PVE-10	10[d]	1.07[d]	265	95[e]	5[e]
PVE-120	120[d]	1.01[d]	273	95[e]	5[e]

[a] Number-average molecular weight by vapor pressure osmometer (VPO) in toluene at 323 K. [b] Molecular weight distribution by size exclusion chromatography (SEC) in THF at 313 K. [c] From ^{13}C NMR. [d] From SEC in THF with multiangle light scattering detector. [e] From ^1H NMR. [f] This sample is perdeuterated.

Polymerizations were carried out in a glass reactor under an inert argon atmosphere. A typical monomer concentration for polymerization was 15 wt %. Isoprene was polymerized at 40 °C for 4 h. A 20-fold molar excess of ethylene oxide was then added to the reactor and allowed to react for 12 h. The reaction was terminated with an excess of a methanol/HCl solution. Butadiene was polymerized in the presence of a 2-fold molar excess of 1,2-dipiperidinoethane at 20 °C for 4 h and was terminated with ethylene oxide and acidic methanol in the same manner as isoprene. The ethylene oxide/acidic methanol termination results in the presence of a single hydroxyl functional group at the end of each chain,[33] which could subsequently be used for attaching a photochromic dye for tracer diffusion measurements by forced Rayleigh scattering. The resulting polymers were washed with water to remove any residual salts and precipitated in a mixture of methanol and 2-propanol. The polymer was then dried under vacuum for at least 1 week, until no solvent peaks were visible in the ^1H NMR spectra.

The molecular weights and molecular weight distributions of the high molecular weight polymers were determined by size exclusion chromatography (SEC) in THF. Separation was achieved by three Phenomenex Phenogel columns with pore sizes of 10^3, 10^4, and 10^5 Å. An interferometric refractometer (Wyatt Technology OPTILAB) and a multiangle light-scattering detector (Wyatt Technology DAWN) positioned downstream of the columns enabled the determination of polymer molecular weights. Refractive index increments of 0.124 and 0.119 mL/g were determined for PI-78 and PVE-120, respectively. The microstructure of each polymer was determined by ^1H NMR. The molecular weights, polydispersities, and microstructures of all polymers are listed in Table 1.

Pulsed-Gradient Spin−Echo NMR. PGSE diffusion experiments in the proton resonance, aided by transverse relaxation measurements, were carried out on a 33 MHz Spin-Lock CPS-2 spectrometer operating with a wide-gap electromagnet. Gradient coils supplied horizontal gradients of calibrated magnitudes decreasing from 710 to 573 G/cm as the temperature was increased between 30.5 and 125 °C. The temperature is controlled to within ±0.2 °C of the set point by the flow of heated air through the NMR−PGSE probe. Principal-echo transverse magnetization decays were nonexponential but unimodal, with T_2 ranging between 12 and 50 ms.

The nonspectroscopic PGSE experiments were performed at fixed G by varying the duration δ of each of the pair of gradient pulses coordinated with the stimulated-echo rf pulse sequence. In this work, the rf pulse spacing τ between the first two 90° pulses was 18 ms, and the spacing between the first and third pulses, and hence also the spacing Δ between the gradient pulses, was 100 ms. To minimize residual gradient effects, Δ was never larger than $\delta - 6$ ms, and usually did not exceed 3 ms. A steady gradient $G_o = 0.35$ G/cm parallel to G was used for convenience in data collection. Between 8 and 12 values of δ were employed to produce a maximal echo attenuation to below 3% of the original echo. Signal averaging of between 5 and 20 passes for each δ improved the signal-to-noise ratio. Experiments were conducted off-resonance by −3 kHz in single-sideband mode with single-phase rf phase-sensitive detection, and the echo signal A was measured as the integral over the magnitude Fourier transform of the beat between echo and reference, after correction for *rms* baseline noise. Several independent checks revealed no explicit dependence of the extracted diffusion coefficient on δ, ensuring that the diffusion was Fickian.

Data reduction was performed off-line by the current PC version of a Fortran program[34] which accounts for residual gradient effects,[35] known polymer polydispersity,[36] and multicomponent diffusion.[36,37] The measured echo attenuation curves reflected a modest, smooth D distribution:

$$\frac{A(X)}{A(0)} = \sum_i^N w_i \exp\left(-\frac{\tau}{T_{2i}}\right) \exp(-\gamma^2 D_i X) \qquad (1)$$

where $X = (G\delta)^2(\Delta - \delta/3)$, with small additional terms in GG_o, and γ denotes the proton gyromagnetic ratio. The normalized sum over $N = 10$ terms simulated a log-normal distribution by coordinating weights w_i with corresponding diffusivities D_i. The two fitted parameters were a mean diffusivity $\langle D \rangle$ and a standard deviation σ_D. The latter never exceeded 20% of $\langle D \rangle$, as expected for modest molecular weight dispersity. The estimated weak dependence of T_2 on molecular weight in the ensemble was also routinely included in the fitted model. The resulting fits were successful in all cases.

Dielectric Relaxation. Dielectric response was measured using a Novocontrol α high-resolution dielectric analyzer. Further details regarding the acquisition and evaluation of data are available elsewhere.[38,39] The measurements were performed in the frequency range from 0.01 Hz to 4 MHz at temperatures between −65 and +30 °C. At all times the temperature was maintained within ±0.1 °C of the set point.

Rheology. Shear moduli measurements were made with an ARES rheometer (Rheometric Scientific) using parallel plate geometry. Both 25 and 7.94 mm diameter plates were employed, depending on the modulus of the material and temperature range of the measurement. All samples were prepared by codissolving polymers with a small amount of 2,6-di-*tert*-butyl-4-methyl-phenol (0.5% by weight) in methylene chloride. The solvent was removed by evaporation, and the samples were annealed for 12 h under vacuum at 70 °C. Two different approaches were adopted for loading samples into the rheometer. Rubbery samples were molded into easily loadable disks under vacuum at 70 °C. Liquidlike samples were loaded with a spatula, and the plates were slowly rotated and brought together until an even loading was achieved. Gap spacings of approximately 1 mm were used for all measurements. The gap width was adjusted at each temperature and a correction for the thermal expansion of the tool set was applied to determine the gap width. The storage (G') and loss (G'') moduli of each sample were determined in the linear viscoelastic regime over temperatures ranging from −40 to +100 °C. The sample was enclosed in a convection oven, and the temperature was controlled by passing nitrogen gas across the sample and tool set. At all times, the sample temperature was maintained within ±0.5 °C of the set point. Zero shear viscosities (η) were extracted in the terminal regime by taking the value of G''/ω as $\omega \to 0$.

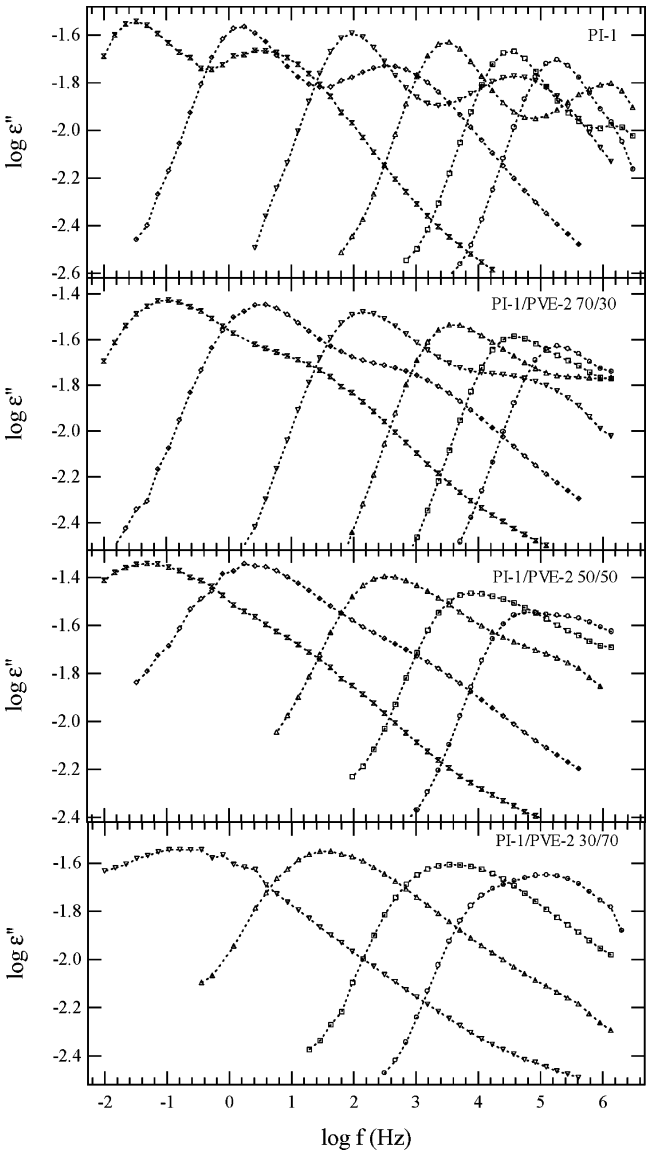

Figure 1. Dielectric loss curves at selected temperatures for pure PI-1 and PI-1/PVE-2 blends. The dashed lines are guides to the eye. The measurement temperatures (K, from left to right) are as follows: (PI) 208, 218, 233, 253, 273, 293; (PI/PVE 70/30) 218, 228, 243, 263, 283, 303; (PI/PVE 50/50) 223, 233, 253, 273, 293; (PI/PVE 30/70) 238, 253, 273, 293.

Results

Dielectric Relaxation. Figure 1 shows the dielectric response (ϵ'' vs f) of pure PI-1 and three PI-1/PVE-2 blends, at a series of temperatures above T_g. The contribution from the sample conductivity at low frequency has been cut off for clarity. For pure PI-1, due to its low molecular weight and narrow molecular weight distribution, two relaxation processes are apparent: a main loss peak at low frequencies, which corresponds to the dielectric normal mode (terminal relaxation of the chain), and a weaker loss peak at high frequencies, corresponding to the segmental dynamics. For blends, the interpretation is more complicated because concentration heterogeneities broaden the dielectric loss peaks, and because both PI-1 and PVE-2 components contribute to the dielectric response (PVE-2 contributes only to the segmental relaxation). As a consequence, not only are the loss peaks broader in the blends than the pure homopolymer but also the segmental relaxation features are blurred. These factors

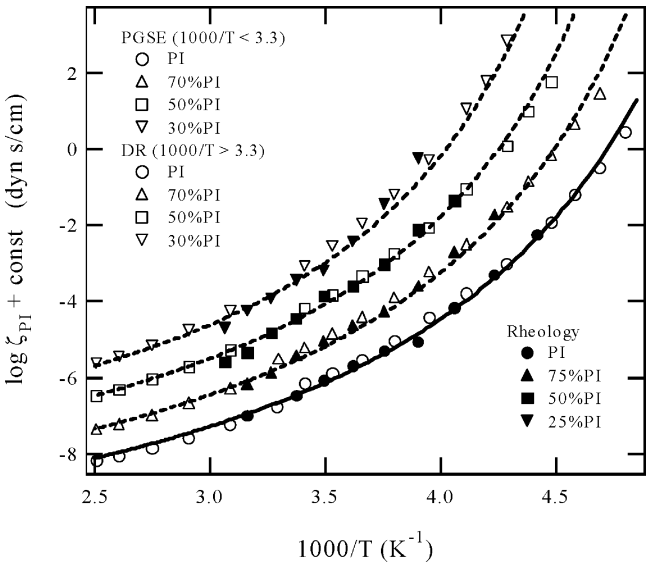

Figure 2. Terminal dynamics of pure PI and PI components in blends with PVE presented as monomeric friction factors. Open symbols are for low molecular weight blends of PI-1/PVE-2 while solid symbols are for high molecular weight blends. The solid line is a VTF fit curve for pure PI. Dashed lines are the prediction for PI components using the Lodge−McLeish model. For viewing purposes, all values for each composition have been vertically shifted by an arbitrary constant. These shift factors are as follows: PI/PVE 70/30, 0.7; PI/PVE 50/50, 1.5; PI/PVE 30/70, 2.2.

modify the shape and strength of the dielectric relaxation, but do not obscure the PI-1 normal mode relaxation. By comparing pure PI-1 with the blends, it is apparent that both segmental and terminal dynamics are strongly affected by mixing. The loss maxima of the blends are progressively shifted toward lower frequencies with increasing PVE content, indicating a slowing down of the PI-1 due to the presence of the PVE-2 chains.

In this work, we are only concerned with the average relaxation times. We take the terminal relaxation time $\tau_1 = 1/(2\pi f_{max})$, where f_{max} is the peak frequency. For pure PI-1 the maximum positions of normal mode and segmental dynamics are clearly separated and we can obtain both. For the PI-1 component in the blends, only the normal mode relaxation could be extracted unambiguously. The terminal dynamics of PI-1 in the various samples can be discussed in terms of the monomeric friction coefficient, $\zeta(\phi,T)$:

$$\zeta = \frac{3\pi^2 kT}{N\langle R^2\rangle}\tau_1 \tag{2}$$

Here N is the degree of polymerization of PI-1, $\langle R^2\rangle$ is the mean square end-to-end distance of the polymer chain (calculated from the characteristic ratio $C_\infty = 4.6$), and the Rouse model has been assumed. These results are shown as a function of temperature in Figure 2 for various compositions, along with other data to be described below.

Pulsed-Gradient Spin−Echo NMR. PGSE is complementary to DR in that it provides access to information about terminal dynamics that lie outside of the frequency window of DR. Diffusion measurements were made on the same samples used for the DR and NMR relaxation experiments.[29] The resulting diffusion coefficients for PI-1 in the pure homopolymer and PI-1/PVE-2 blends are listed in Table 2. (Only PI-1 diffusion is observed due to the deuteration of the PVE-2). These data show the expected effects of blending: D increases with PI-1 content at fixed temperature, and the temperature dependence of D becomes stronger with increasing PVE-2 content. For comparison purposes, we also transformed D to the monomeric friction coefficient ζ and terminal relaxation time τ_1 using the Rouse model:

Table 2. Diffusion Coefficients for Pure PI-1 and PI-1 in PI-1/PVE-2

temp (°C)	log D (cm²/s)			
	PI-1	70% PI-1	50% PI-1	30% PI-1
30.5	−7.91	−8.34		
50.5	−7.41	−7.67	−7.87	−8.19
70.5	−7.03	−7.26	−7.41	−7.67
90.5	−6.73	−6.91	−7.05	−7.24
110.5	−6.51	−6.66	−6.76	−6.92
125.5	−6.37	−6.5	−6.58	−6.73

$$\zeta = \frac{kT}{ND} \tag{3}$$

$$\tau_1 = \frac{\langle R^2\rangle}{3\pi^2 D} \tag{4}$$

The monomeric friction coefficients of PI-1 obtained in this way are plotted in Figure 2 as open symbols together with DR data. The agreement between the two techniques is excellent, lending support to the applicability of the Rouse model in this case.

Rheology. Time−temperature superposition was employed to obtain master curves of G' and G'' for PI-78, PI-22, PVE-120, and PVE-10. Horizontal shift factors (a_T) were determined by shifting until superposition of $\tan|\delta|$ was observed. PI samples required a small vertical shift, consistent with a prior report,[25] whereas no vertical shift was necessary for PVE samples. The creation of master curves for the blends was also attempted, and the failure of time−temperature superposition was evident. As such failure of time−temperature superposition for PI/PVE blends is well documented,[4,19,23] these results are not shown.

Plateau moduli (G_N^o) for the homopolymers and the blends were estimated from the plateau region of the frequency sweep results; G_N^o was taken as the value of G' at the frequency of the local minimum in G''.[40] The values of G_N^o for PI-78 and PVE-120 were similar to those reported previously.[25] No plateau moduli could be determined in this manner for PI-22 or PVE-10, as no local minimum in G'' was present. G_N^o was determined as a function of composition from PI-78/PVE-120 blends.

Two methods were used to determine the longest relaxation time (τ_1) for the homopolymer samples. For temperatures where G' and G'' intersect, τ_1 was taken as the reciprocal of the crossover frequency. At higher temperatures where terminal behavior was observed, τ_1 was determined from η using the following reptation relation:[41]

$$\eta = \frac{\pi^2}{12} G_N^o \tau_1 \tag{5}$$

Where both methods could be applied, there was good agreement between the τ_1 values obtained.

The values of τ_1 for each blend component were extracted by fitting G' and G'' data via the Tsenoglou

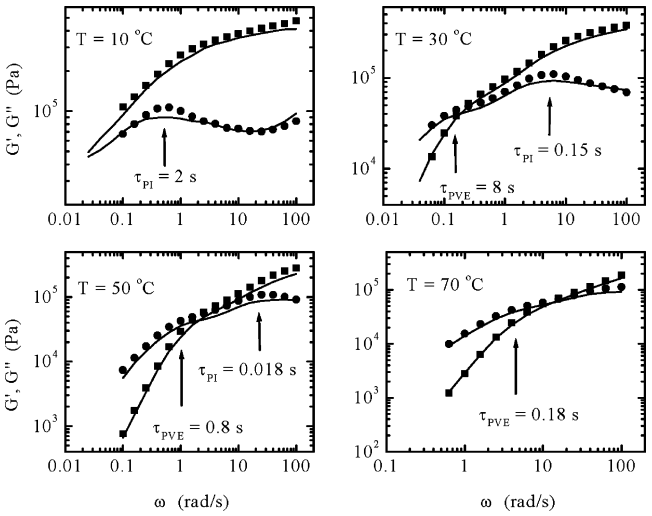

Figure 3. Application of modified Tsenoglou model to G' (■) and G'' (●) for a 50/50 PI-78/PVE-120 blend. The longest relaxation time for each blend component is labeled at $\omega = 1/\tau_1$.

entanglement model.[42] An approximate form of this model was developed and fit to blends of PI-78/PVE-120, PI-78/PVE-10, and PI-22/PVE-120, as described in the Appendix. Representative fits of this approximate Tsenoglou model to a 50/50 blend of PI-78/PVE-120 at selected temperatures are shown in Figure 3. We estimate the uncertainty in τ_1 by this method to be significantly less than a factor of 2.

Extraction of $\zeta(\phi,T)$ from $\tau_1(\phi,T)$. Previous workers have used a reptation-based equation to extract ζ from τ_1 for miscible polymer blends.[23,25] One such relationship is[41]

$$\tau_1 = \frac{15}{24\pi^2}\frac{\zeta b^2}{k_B T}\left(\frac{M}{M_e}\right)\left(\frac{M}{M_o}\right)^2 \quad (6)$$

where b is the polymer statistical segment length, M_e is the entanglement molecular weight, and M_o is the molecular weight of the repeat unit. Equation 6 assumes that the relationship between τ_1 and the molecular weight (M) follows the scaling law $\tau_1 \sim M^3$, whereas the experimentally established scaling relationship between τ_1 and M is approximately $\tau_1 \sim M^{3.4}$.[43] To properly account for the experimental molecular weight dependence of τ_1, the reptation relationship between τ_1 and ζ was therefore modified to yield

$$\tau_1 = \frac{15}{24\pi^2}\frac{\zeta b^2}{k_B T}\left(\frac{M}{M_e}\right)^{1.4}\left(\frac{M}{M_o}\right)^2 \quad (7)$$

The entanglement molecular weight of each blend was determined using the relationship[43]

$$G_N^o = \frac{\rho R T}{M_e} \quad (8)$$

where ρ is the appropriately weighted mass density. This approach assumes a single value of M_e for both components in the blend. This differs from the approach taken by Kornfield and co-workers,[25] where a unique M_e for each blend component was assigned. Quantitatively, the difference between the two approaches matters little, as the individual M_e values for each blend component reported by Kornfield and co-workers are essentially the same.[25]

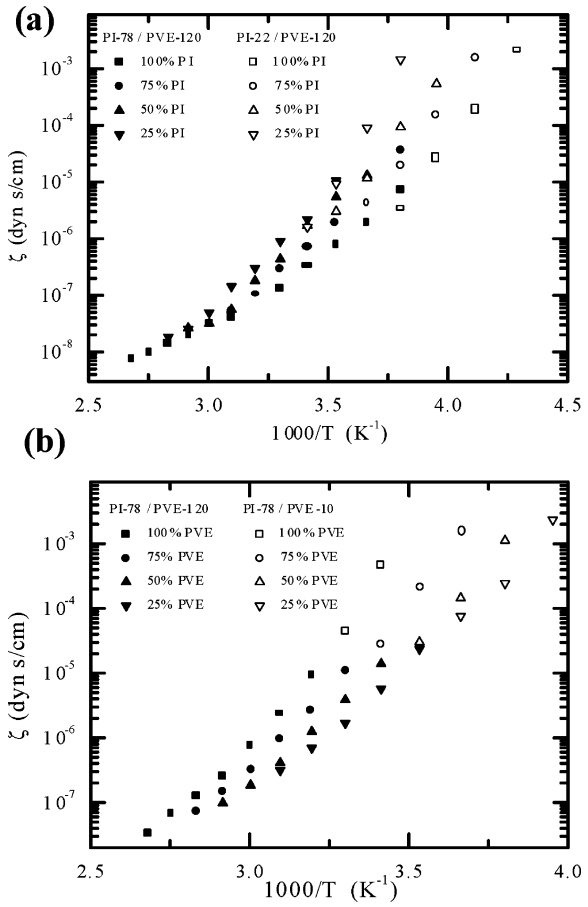

Figure 4. ζ extracted from rheology experiments for (a) PI and (b) PVE. The filled symbols represent ζ determined from PI-78 and PVE-120 and the open symbols depict ζ obtained from PI-22 and PVE-10.

Values for $\zeta(\phi,T)$ for both PI and PVE were determined using eq 7. The values of τ_1 for the slower relaxing component in blends where the two relaxation times were widely separated (i.e., PI in PI-78/PVE-10 and PVE in PI-22/PVE-120) were not used to determine ζ, as the data could possibly be affected by constraint release contributions.[44] Some evidence for constraint release was indeed observed, as τ_1 for PI-78 in blends with PVE-10 was approximately a factor of 2 less than τ_1 for PI-78 in blends with PVE-120. The τ_1 values for both components in the PI-78/PVE-120 blends could be used for the determination of ζ.

Parts a and b of Figure 4 show $\zeta(\phi,T)$ extracted from $\tau_1(\phi,T)$ for PI and PVE, respectively. The use of two different molecular weights for PI and PVE enables the determination of ζ over a wider range of temperatures. For both PI and PVE, ζ obtained from the high and low molecular weight polymers agree well. This agreement implies that ζ is independent of molecular weight over the range of molecular weights examined, lending support for the applicability of eq 7.

ζ values for PI extracted from rheology data are plotted in Figure 2. A temperature shift of 8 K has been applied to the rheology data to account for the T_g differences between PI-1 and PI-78. Clearly, ζ values extracted from rheology measurements agree quantitatively with ζ values determined by DS and PGSE.

Comparison of $\zeta(\phi,T)$ to Published Results. Previous studies of $\zeta(\phi,T)$ for PI/PVE blends can be found

in the literature. Our data were compared to those provided by the rheo-optic studies of Zawada and co-workers[23] and of Kornfield and co-workers.[25] The approaches used to extract ζ in these previous studies differ in some subtle details from that taken here. The results of the previous investigations were adjusted to account for these differences, and the resulting ζ values were then compared. The three data sets agree quantitatively (results not shown), with a few minor exceptions. For example, the results of Zawada and co-workers tend to depart slightly from the other two data sets at low component concentrations. Also, our data differ from the data of Kornfield and co-workers at higher temperatures for all compositions, including homopolymers. For example, our values of ζ are roughly a factor of 2−4 greater for temperatures above 60 °C. This difference is actually relatively modest, considering that ζ varies over many orders of magnitude over the temperature range examined.

Discussion

Comparison of Terminal and Segmental Dynamics. The results described above enable a direct comparison of the composition and temperature dependence of the terminal relaxation of polymer chains with the dynamics of local motions along the chain backbone. The friction factor ζ reflects the terminal dynamics, in a model-dependent way, whereas the segmental relaxation time is a direct measure of the rate of local backbone relaxation processes. Current theories of homopolymer melt dynamics (e.g., Rouse, reptation) consider large-scale chain motion to be driven by shorter length scale motions. Thus, in the Rouse model, all relaxation times depend linearly on the bead friction coefficient. This is consistent with the experimental observation that sufficiently far above T_g segmental and terminal dynamics in homopolymer melts generally have the same temperature dependences. For example, Adachi and Hirano showed that the terminal and segmental times for PI have the same temperature dependence down to $T_g + 20$ °C and that they differed by only 0.3 log units at $T_g + 10$ °C.[45] Here we test whether a single effective friction coefficient controls both the segmental and terminal dynamics for a given homopolymer in a blend; i.e., we ask whether the segmental and terminal dynamics have the same temperature and composition dependence. Previously published results for segmental relaxation times[11,28,29] can be compared with either ζ/T or τ_1, as ζ/T and τ_1 are equivalent in terms of their composition and temperature dependences. The average segmental relaxation time will be denoted $\tau_{seg,c}$.

The terminal and segmental dynamics of PI for homopolymers and blends are compared in Figure 5. The τ_1 measurements from PGSE and DR were shifted vertically by a single composition-independent shift factor, to account for the unknown proportionality factor between the measured segmental relaxation time and τ_1. A temperature shift of 8 K has been applied to the high molecular weight data, to account for the difference in homopolymer values of T_g. The good agreement between the various data sets demonstrates that the temperature and composition dependence of both the segmental and terminal dynamics is essentially the same for PI in all the blends. While only low molecular weight τ_1 data are shown in Figure 5, the results in Figure 2 indicate that this conclusion applies to all molecular weights examined.

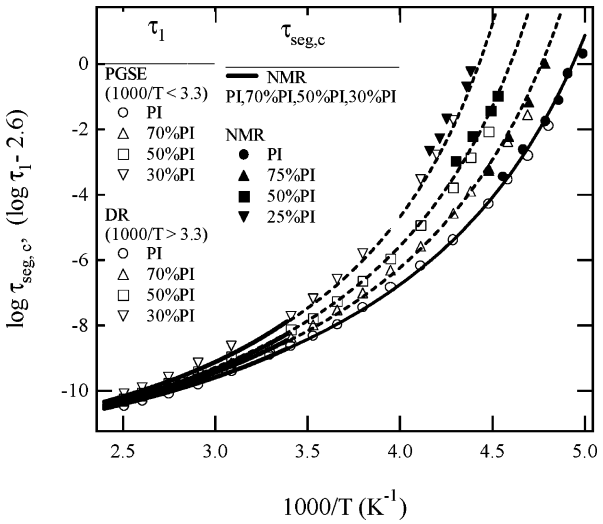

Figure 5. Comparison of the terminal and segmental dynamics for PI and PI components in blends. Solid symbols are the results of Kornfield and co-workers[28] while heavy solid lines come from Min et al.'s work on PI-1/PVE-2 blends.[29] The thin solid line is a VTF fit curve for pure PI over the whole temperature range based on the segmental dynamics measured from liquid-state NMR, DR (not shown), and solid-state NMR. The parameters used are as follows: $\tau_\infty = 0.28$ ps, $B = 510$ K, $T_0 = 162$ K. Dashed lines are the predicted segmental relaxation times for PI components using the Lodge−McLeish model, with $\phi_s(\mathrm{PI}) = 0.40$.

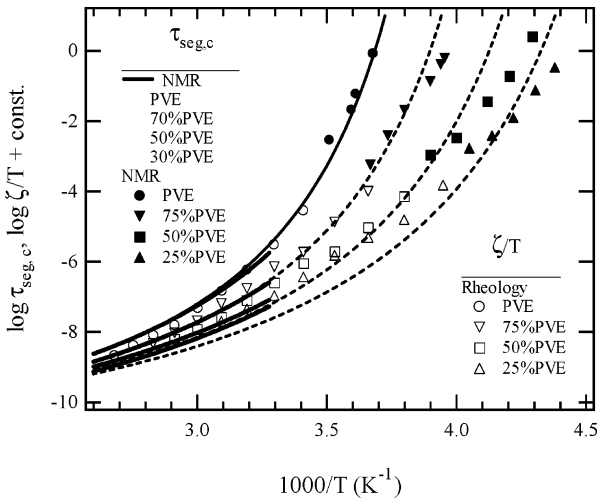

Figure 6. Comparison of the terminal and segmental dynamics for PVE and PVE components in blends. Filled symbols are the results of Kornfield and co-workers,[28] heavy solid lines come from Min et al.'s work on PI-1/PVE-2 blends,[29] and open symbols are the rheological results on the high molecular weight blends. The thin solid line is a VTF fit curve for pure PVE over the whole temperature range based on the segmental dynamics measured from liquid and solid-state NMR. The parameters used are as follows: $\tau_\infty = 4.8$ ps, $B = 400$ K, $T_0 = 225$ K. Dashed lines are the predicted segmental relaxation times for PVE components using the Lodge−McLeish model, with $\phi_s(\mathrm{PVE}) = 0.20$. The vertical shift factor was 1.3.

Figure 6 shows the analogous comparison between terminal and segmental dynamics for PVE. Again, only a single vertical shift factor was used for all compositions. A temperature shift of 11 K has been applied to the low molecular weight data, to account for the difference in homopolymer values of T_g. As with PI, the temperature and composition dependence of the dynamics was found to be equivalent on both the terminal and segmental levels. This result is consistent with previous

work by Kornfield and co-workers, and extends their observations to a wider range of temperatures and molecular weights.[28]

The success of this comparison for both blend components suggests that any complication that arises in the composition and temperature dependence of terminal dynamics in PI/PVE blends, such as the failure of time−temperature superposition, can be attributed entirely to local effects. The polymer motion on the length scale of the entire chain tracks the segmental dynamics, without the introduction of any additional complexity. These results also suggest that any model that successfully describes the segmental dynamics for PI/PVE blends will also be applicable to terminal dynamics. Finally, these results provide further justification for applying standard chain dynamics models to miscible blends, once $\zeta(\phi,T)$ is known for both components.

Lodge−McLeish Model. The model of Lodge and McLeish (L−M) provides a framework for predicting $\tau_{seg,c}(\phi,T)$ and therefore $\zeta(\phi,T)$ at temperatures sufficiently far above T_g. There are several basic assumptions upon which this model relies. The segmental relaxation process is postulated to be characterized by conformational relaxations on the scale of a Kuhn segment. The rate of this relaxation process is affected by the local concentration in the surrounding region. The volume (V) of this region is therefore taken to be $V \approx l_k^3$, where l_k is the Kuhn length. Chain connectivity leads to an excess of monomers of the blend component of interest within V, relative to the bulk concentration. Because of the small size of V, this effective concentration ($\phi_{eff,A}$) of monomers of type A can deviate significantly from the bulk composition ϕ. $\phi_{eff,A}$ is calculated with the relation[12]

$$\phi_{eff,A} = \phi_{s,A} + (1 - \phi_{s,A})\phi \tag{9}$$

where $\phi_{s,A}$ is the "self-concentration" of monomers of type A. A similar relation applies for component B. ϕ_s is the volume fraction of V occupied by a Kuhn length's worth of monomers, determined by the relationship[12]

$$\phi_s = \frac{C_\infty M_o}{k\rho N_{av} V} \tag{10}$$

where k is the number of backbone bonds per repeat unit and N_{av} is Avogadro's number. As Lodge and McLeish note, eq 10 could easily incorporate a prefactor of order unity, as the choice of $V = l_k^3$ is somewhat arbitrary. Also, it may be helpful to recognize that ϕ_s thus defined is equal to the ratio of the packing length, p,[46] divided by the Kuhn length.

In the L−M framework, each blend component experiences a distinct effective glass transition temperature ($T_{g,eff}$) that depends on ϕ_{eff}. We assume that $T_{g,eff}$ for component A can be determined from ϕ_{eff} via the Fox relation:

$$\frac{1}{T_{g,eff}} = \frac{\phi_{eff}}{T_{g,A}} + \frac{1 - \phi_{eff}}{T_{g,B}} \tag{11}$$

where $T_{g,A}$ and $T_{g,B}$ are the glass transition temperatures of (unmixed) components A and B. Figure 7 shows values for $T_{g,eff}$ for PI and PVE calculated using the calorimetric glass transition temperatures from Table 1 and the Kuhn lengths extracted from literature values for chain dimensions.[46] These results will be discussed further subsequently.

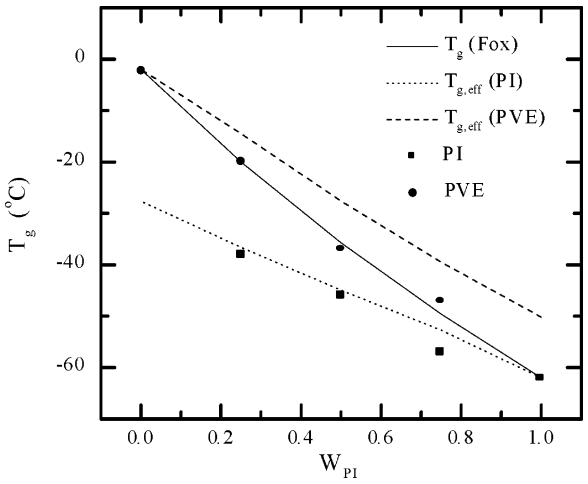

Figure 7. Lodge−McLeish predictions for the effective glass transition temperature for each component in a PI/PVE blend as a function of composition. The solid line is the Fox prediction for the T_g of the blend, while the dashed lines are the predicted $T_{g,eff}$ for each component. The solid data points are experimental estimates of $T_{g,eff}$ taken from ref 28.

The next important assumption is that $\tau_{seg,c}(\phi,T)$ can be calculated from $T_{g,eff}$ via the Vogel−Fulcher−Tammann (VFT) equation

$$\log\left(\frac{\tau_{seg,c}(\phi,T)}{\tau_\infty}\right) = \frac{B}{T - (T_o + T_{g,eff}(\phi_{eff}) - T_g)} \tag{12}$$

where τ_∞, B, and T_o are VFT parameters obtained from fitting homopolymer data, and T_g is the homopolymer glass transition temperature. An analogous relation is used to calculate $\zeta(\phi,T)$. In this approach the assumption is made that τ_∞, B, and T_o are independent of composition, and that therefore all of the composition dependence of $\tau_{seg,c}$ is accounted for by the composition dependence of $T_{g,eff}$. Similarly if the Williams−Landel−Ferry equation were used in place of eq 12, the relevant parameters C_1^g, C_2^g and $\tau_{seg,c}(T_g)$ would be taken to be independent of composition. Note that a single VFT or WLF relation may not always describe the temperature dependence over a very wide temperature range, such as employed here. In such a case, a more elaborate relation than eq 12 could be used.

Comparison of $\tau_{seg,c}$ and ζ with the L−M Model. The data in Figures 2, 5, and 6 for $\tau_{seg,c}(\phi,T)$ and $\zeta(\phi,T)$ were fit to the L−M model using the approach outlined above, with ϕ_s for each component treated as a fitting parameter. For PI ϕ_s was taken to equal 0.4, which corresponds to a self-concentration length scale ($V^{1/3}$) of 7 Å. For PVE, $\phi_s = 0.2$, and therefore $V^{1/3} = 12$ Å. The Kuhn segment lengths for PI and PVE are 6.8 and 11.6 Å respectively, and thus the fitting values of $V^{1/3}$ are in fact very close to the Kuhn segment lengths.

Figures 2 and 5 show comparisons between the fits to the L−M model (smooth curves) and the experimental data for PI. The L−M model quantitatively (i.e., within a factor of 2) describes the dynamics of PI over the entire range of temperatures and compositions examined. Figure 6 shows the comparison between the model and experiment for PVE. The agreement for PVE is not quite quantitative, but the general trends of the temperature and composition dependence of the dynamics of PVE are effectively captured by the L−M model.

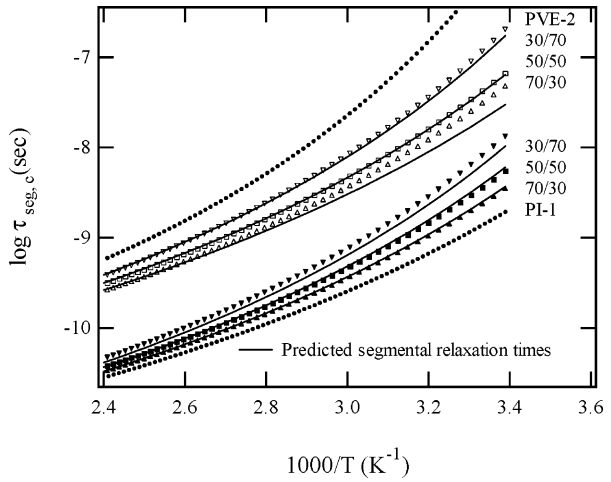

Figure 8. Comparison of the PI and PVE component segmental dynamics in PI-1/PVE-2 blends to the Lodge−McLeish model prediction. The segmental relaxation times based upon NMR measurements (dotted lines and markers) come from Min et al.'s work.[29] Here we used $\phi_s(\mathrm{PI}) = 0.45$ and $\phi_s(\mathrm{PVE}) = 0.25$ in the model calculation.

At this point, a note about the sensitivity of the dependence of $\tau_{seg,c}$ on $V^{1/3}$ is in order. A relatively small change in the value of $V^{1/3}$ can result in a large change in the predicted value of $\tau_{seg,c}$, particularly at temperatures that are close to $T_{g,eff}$. As an example of this sensitivity, one can examine predictions of $\tau_{seg,c}$ for PVE in a 50% blend of PI and PVE. A reduction of $V^{1/3}$ by 20% would increases the value of $T_{g,eff}$ by 6.5 °C. At −10 °C this 20% decrease in $V^{1/3}$ results in an order of magnitude increase in $\tau_{seg,c}$. The sensitivity of the dependence of $\tau_{seg,c}$ on $V^{1/3}$ increases as the temperature approaches $T_{g,eff}$.

The L−M model was fit separately to published high-temperature NMR $\tau_{seg,c}$.[29] This fit is shown in Figure 8. The best fit to these data was obtained using slightly higher values for ϕ_s; $\phi_s = 0.45$ for PI, and $\phi_s = 0.25$ for PVE. These choices correspond to values of $V^{1/3}$ which are identical to the Kuhn lengths for each component. The L−M model therefore successfully predicts the composition and temperature dependence of segmental dynamics for each component in the PI/PVE blends over a temperature range of roughly 20 to 140 °C, using the Kuhn length as the self-concentration length scale.

The successful comparisons between the L−M model and the data in Figures 2, 5, 6, and 8 are achieved with a length scale that is independent of temperature. However, it is worth considering the possibility that the length scale for the self-concentration does increase weakly with decreasing temperature. As noted in the Introduction, several related models postulate an increasing "cooperativity" length scale for dynamics as T_g is approached.[15,16,47] In the context of the L−M model, such an effect would lead to a reduction in ϕ_s on approaching $T_{g,eff}$. An increase of $V^{1/3}$ with decreasing temperature could be consistent with the observation that higher temperature data (Figure 8) are better fit with a value of ϕ_s that is slightly greater than the value obtained from fitting over the entire temperature range. This proposed temperature dependence for $V^{1/3}$ might also account in part for the difference between the L−M model and the PVE data in Figure 6. Qualitatively, the NMR data for $\tau_{seg,c}$ of PVE at low temperatures also appear to have a weaker temperature dependence than the L−M model prediction. A decrease in ϕ_s at lower temperatures would result in a reduction of $T_{g,eff}$ and would weaken the temperature dependence of $\tau_{seg,c}$.

Low-temperature $\tau_{seg,c}$ measurements were used previously to estimate $T_{g,eff}$ for both PI and PVE as a function of composition.[28] These estimates are plotted in Figure 7. For PI, $T_{g,eff}$ thus determined falls on the line corresponding to the Lodge−McLeish prediction of $T_{g,eff}$, whereas for PVE the predicted $T_{g,eff}$ is somewhat higher than the experimental results. In fact, $T_{g,eff}$ for PVE is in good agreement with the Fox prediction of the T_g of the blend, i.e., the values that would be obtained as ϕ_s tends to zero. In the end, however, although the data presented here might lend some support to the notion of a temperature-dependent length scale, they also suggest that this would be at most a relatively minor effect compared to the self-concentration calculated on the scale of the Kuhn length.

Summary

Both terminal and segmental dynamics of each component in miscible PI/PVE blends have been examined by a variety of experimental techniques. The longest relaxation times, determined by rheology (PI and PVE), pulsed field-gradient NMR (PI), and dielectric relaxation (PI), are consistently interpreted in terms of the monomeric friction factor, ζ, using either the Rouse or reptation model, as appropriate. A modification of the Tsenoglou mixing rule[42] was developed and applied to facilitate extraction of the longest relaxation time of each component from the viscoelastic moduli. Segmental relaxation processes monitored directly by liquid state NMR (higher temperatures) and by solid state NMR (lower temperatures) reported previously are also compared with ζ. The combined data encompass the complete composition range, and a temperature interval of almost 200 K. The results are compared with the predictions of the Lodge−McLeish model, which places particular emphasis on self-concentrations calculated on the basis of a temperature-independent length scale, comparable to the Kuhn length of the component in question. The principal conclusions are as follows:

1. For the PI component at each composition studied, values of ζ obtained agreed well among the various techniques, and for both PI and PVE, ζ was sensibly independent of molecular weight.

2. For each component the ratio of the longest relaxation time to the segmental relaxation time is independent of both temperature and composition. This result, and the previously cited one, suggest that standard chain dynamics models should be applicable to athermal miscible blends.

3. The Lodge−McLeish model provides a quantitative description of the PI dynamics over the entire composition and measured temperature range, via a temperature-independent length scale very close to the Kuhn length. In this approach, no new parameters are invoked, beyond those required to describe pure polymer dynamics.

4. The Lodge−McLeish model is somewhat less successful in describing the PVE dynamics quantitatively, but it still captures both the trends and the relative magnitudes of the composition and temperature dependences very well.

The nature of the deviations between the Lodge−McLeish model and the results for PVE might be taken to suggest the relevance of a temperature-dependent

length scale; this issue will require further examination. Similarly, the encouraging success of this simple model in describing one particular system hints that comparisons to data for other model blends should be fruitful.

Acknowledgment. This work was supported in part by the National Science Foundation, through Award DMT-9901087 (T.P.L.) and through Award DMR-0099849 (M.D.E.).

Appendix

In this appendix, we present an approximate form for the Tsenoglou entanglement model, as applied to miscible blends. For an entangled binary miscible polymer blend of components a and b, the Tsenoglou model predicts that the stress relaxation modulus ($G(t)$) is given by the relation:[42]

$$G(t) = \phi_a^2 G_a(t,\phi,T) + \phi_b^2 G_b(t,\phi,T) + 2\phi_a\phi_b\sqrt{G_a(t,\phi,T)G_b(t,\phi,T)} \quad \text{(A-1)}$$

where ϕ_a and ϕ_b are the volume fractions of components a and b, and G_a and G_b are the stress relaxation moduli of each component in the blend.

To facilitate transformation into the frequency domain, the Tsenoglou model was approximated in the following manner. If $G_a(t)$ and $G_b(t)$ are each treated as single-exponential relaxation functions and components a and b are specified such that $\tau_{1,a} \leq \tau_{1,b}$, one can write the approximation

$$\sqrt{G_a(t)G_b(t)} \approx \sqrt{G^o_{N,a}G^o_{N,b}}\exp\left(\frac{-t/x}{\tau_{1,a}}\right) \quad \text{(A-2)}$$

where x is defined by the equation

$$x = \frac{2}{1+\tau_{1,a}/\tau_{1,b}} \quad \text{(A-3)}$$

The approximation of treating $G_a(t/x)$ as a single exponential is then applied, resulting in the relation

$$\sqrt{G_a(t)G_b(t)} \approx \sqrt{G^o_{N,a}G^o_{N,b}}\frac{G_a(t/x)}{G^o_{N,a}} \quad \text{(A-4)}$$

The approximation in eq A-4 was tested extensively. $G_a(t)/G^o_{N,a}$ and $G_b(t)/G^o_{N,b}$ were simulated over a wide range of $\tau_{1,a}$ and $\tau_{1,b}$ values with the Doi−Edwards constitutive equation. The right and left sides of eq A-4 were compared and found to be in quantitative agreement for all of the simulated data sets. On the basis of this analysis, eq A-4 was deemed an acceptable approximation.

Application of eq A-4 to eq A-1 and subsequent Fourier transformation results in the mixing rule for G':

$$G'(\omega) = \phi_a^2 G'_a(a_{T,a}\omega) + \phi_b^2 G'_b(a_{T,b}\omega) + 2\phi_a\phi_b\sqrt{\frac{G^o_{N,b}}{G^o_{N,a}}}G'_a(a_{T,a}x\omega) \quad \text{(A-5)}$$

where $a_{T,a}$ and $a_{T,b}$ are temperature-and composition-dependent shift factors for blend components a and b. A similar relation exists for G'':

$$G''(\omega) = \phi_a^2 G''_a(a_{T,a}\omega) + \phi_b^2 G''_b(a_{T,b}\omega) + 2\phi_a\phi_b\sqrt{\frac{G^o_{N,b}}{G^o_{N,a}}}G''_a(a_{T,a}x\omega) \quad \text{(A-6)}$$

Equations A-5 and A-6 were used to fit G' and G'' data for blends of PI-78/PVE-120, PI-78/PVE-10, and PI-22/PVE-120. Homopolymer master curves shifted to a reference temperature of 20 °C were used as the functions $G'_a(\omega)$ and $G'_b(\omega)$. The component shift factors $a_{T,a}$ and $a_{T,b}$ in eq A-5 and eq A-6 were then adjusted until the best fit to the experimental data was obtained. The value of τ_1 for each blend component was determined from the component shift factor with the relation

$$\tau_{1,i}(\phi_i,T) = \frac{\tau_1(\phi_i=1,T=20°C)}{a_{T,i}(\phi,T)} \quad \text{(A-7)}$$

where i denotes the blend component.

References and Notes

(1) Minnick, M. G.; Schrag, J. L. *Macromolecules* **1980**, *13*, 1690−1695.
(2) Colby, R. H. *Polymer* **1989**, *30*, 1275−1278.
(3) Roovers, J.; Toporowski, P. M. *Macromolecules* **1992**, *25*, 1096−1102.
(4) Roovers, J.; Toporowski, P. M. *Macromolecules* **1992**, *25*, 3454−3461.
(5) Pathak, J. A.; Colby, R. H.; Floudas, G.; Jerome, R. *Macromolecules* **1999**, *32*, 2553−2561.
(6) Trask, C. A.; Roland, C. M. *Macromolecules* **1989**, *22*, 256−261.
(7) Composto, R. J.; Kramer, E. J.; White, D. M. *Polymer* **1990**, *31*, 2320−2328.
(8) Green, P. F.; Adolf, D. B.; Gilliom, L. R. *Macromolecules* **1991**, *24*, 3377−3382.
(9) Kim, E.; Kramer, E. J.; Osby, J. O. *Macromolecules* **1995**, *28*, 1979−1989.
(10) Miller, J. B.; McGrath, K. J.; Roland, C. M.; Trask, C. A.; Garroway, A. N. *Macromolecules* **1990**, *23*, 4543−4547.
(11) Chung, G. C.; Kornfield, J. A.; Smith, S. D. *Macromolecules* **1994**, *27*, 964−973.
(12) Lodge, T. P.; McLeish, T. C. B. *Macromolecules* **2000**, *33*, 5278−5284.
(13) Gell, C. B.; Krishnamoorti, R.; Kim, E.; Graessley, W. W.; Fetters, L. J. *Rheol. Acta* **1997**, *36*, 217−228.
(14) Katana, G.; Fischer, E. W.; Hack, T.; Abetz, V.; Kremer, F. *Macromolecules* **1995**, *28*, 2714−2722.
(15) Kumar, S. K.; Colby, R. H.; Anastasiadis, S. H.; Fytas, G. *J. Chem. Phys.* **1996**, *105*, 3777−3788.
(16) Kamath, S.; Colby, R. H.; Kumar, S. K.; Karatasos, K.; Floudas, G.; Fytas, G.; Roovers, J. E. L. *J. Chem. Phys.* **1999**, *111*, 6121−6128.
(17) Salaniwal, S.; Kant, R.; Colby, R. H.; Kumar, S. K. *Macromolecules* **2002**, *35*, 9211−9218.
(18) Ngai, K. L.; Rendell, R. W.; Rajagopal, A. K.; Teitler, S. *Ann. N.Y. Acad. Sci.* **1986**, *484*, 150−184.
(19) Roland, C. M.; Ngai, K. L. *Macromolecules* **1991**, *24*, 2261−2265.
(20) Roland, C. M.; Ngai, K. L. *J. Rheol.* **1992**, *36*, 1691−1706.
(21) Alegria, A.; Colmenero, J.; Ngai, K. L.; Roland, C. M. *Macromolecules* **1994**, *27*, 4486−4492.
(22) Roland, C. M. *J. Polym. Sci., Part B: Polym. Phys.* **1988**, *26*, 839−856.
(23) Zawada, J. A.; Fuller, G. G.; Colby, R. H.; Fetters, L. J.; Roovers, J. *Macromolecules* **1994**, *27*, 6861−6870.
(24) Arendt, B. H.; Kannan, R. M.; Zewail, M.; Kornfield, J. A.; Smith, S. D. *Rheol. Acta* **1994**, *33*, 322−336.
(25) Arendt, B. H.; Krishnamoorti, R.; Kornfield, J. A.; Smith, S. D. *Macromolecules* **1997**, *30*, 1127−1137.
(26) Arbe, A.; Alegria, A.; Colmenero, J.; Hoffmann, S.; Willner, L.; Richter, D. *Macromolecules* **1999**, *32*, 7572−7581.
(27) Hoffmann, S.; Willner, L.; Richter, D.; Arbe, A.; Colmenero, J.; Farago, B. *Phys. Rev. Lett.* **2000**, *85*, 772−775.

(28) Chung, G. C.; Kornfield, J. A.; Smith, S. D. *Macromolecules* **1994**, *27*, 5729−5741.
(29) Min, B.; Qiu, X.; Ediger, M. D.; Pitsikalis, M.; Hadjichristidis, N. *Macromolecules* **2001**, *34*, 4466−4475.
(30) Tomlin, D. W.; Roland, C. M. *Macromolecules* **1992**, *25*, 2994−2996.
(31) Bywater, S.; Mackerron, D. H.; Worsfold, D. J.; Schue, F. *J. Polym. Sci., Part A: Polym. Chem.* **1985**, *23*, 1997−2003.
(32) Gilman, H.; Cartledge, F. K. *J. Organomet. Chem.* **1964**, *2*, 447−454.
(33) Hillmyer, M. A.; Bates, F. S. *Macromolecules* **1996**, *29*, 6994−7002.
(34) Von Meerwall, E. D.; Ferguson, R. D. *Comput. Phys. Commun.* **1981**, *21*, 421−429.
(35) Von Meerwall, E.; Kamat, M. *J. Magn. Reson.* **1989**, *83*, 309−323.
(36) Von Meerwall, E.; Palunas, P. *J. Polym. Sci., Part B: Polym. Phys.* **1987**, *25*, 1439−1457.
(37) Shim, S. E.; Parr, J. C.; von Meerwall, E.; Isayev, A. I. *J. Phys. Chem. B* **2002**, *106*, 12072−12078.
(38) Fitz, B.; Andjelic, S.; Mijovic, J. *Macromolecules* **1997**, *30*, 5227−5238.
(39) Mijovic, J.; Miura, N.; Monetta, T.; Duan, Y. *Polym. News* **2001**, *26*, 251.
(40) Kannan, R. M.; Lodge, T. P. *Macromolecules* **1997**, *30*, 3694−3695.
(41) Doi, M.; Edwards, S. F. *The Theory of Polymer Dynamics*; Oxford University Press: Oxford, England, 1986.
(42) Tsenoglou, C. *New Trends Phys. Phys. Chem. Polym. [Proc. Int. Symp.]* **1989**, 375−383.
(43) Ferry, J. D. *Viscoelastic Properties of Polymers*, 3rd ed.; John Wiley & Sons: New York, 1980.
(44) Struglinski, M. J.; Graessley, W. W. *Macromolecules* **1985**, *18*, 2630−2643.
(45) Adachi, K.; Hirano, H. *Macromolecules* **1998**, *31*, 3958−3962.
(46) Fetters, L. J.; Lohse, D. J.; Richter, D.; Witten, T. A.; Zirkel, A. *Macromolecules* **1994**, *27*, 4639−4647.
(47) Colby, R. H. *Phys. Rev. E: Stat. Phys., Plasmas, Fluids* **2000**, *61*, 1783−1792.

MA034414Z